RSC Advances

A Facile Hydrothermal Method for Controllable Synthesis of TiO2 Nanocrystals with Tunable Shapes

Journal:	*RSC Advances*
Manuscript ID	RA-ART-07-2015-013006.R2
Article Type:	Paper
Date Submitted by the Author:	06-Nov-2015
Complete List of Authors:	Nie, shengcao; Wuhan University of Technology, Key Laboratory of Silicate Materials Science and Engineering Zhao, Xiujian; Wuhan University of Technology, Key Laboratory of Silicate Materials Science and Engineering liu, baoshun; Wuhan university of technology, School of material science and engineering
Subject area & keyword:	Nanomaterials - Materials < Materials

Journal Name

RSCPublishing

ARTICLE

A Facile Hydrothermal Method for Controllable Synthesis of TiO$_2$ Nanocrystals with Tunable Shapes

Cite this: DOI: 10.1039/x0xx00000x

Received 00th January 2012,
Accepted 00th January 2012

DOI: 10.1039/x0xx00000x

www.rsc.org/

Shengcao Nie, Xiujian Zhao, and Baoshun Liu*

The controllable preparation of anatase TiO$_2$ nanocrystals with tunable shapes has drawn much attention recently. The general method to prepare such nano-TiO$_2$ involves the use of HF as a surfactant. However, the use of HF is top-risk, which should be avoided in experiments. Therefore, the development of facile and friendly methods to controllably synthesize anatase TiO$_2$ nanocrystals is important. In this research, instead of the general titanium precursors, titanium peroxide sol was used as the source material to synthesize anatase TiO$_2$ nanocrystals due to its high stability in water. Oleic acid and oleylamine were used as capping surfactants, a hydrothermal method without using top-risk HF was developed to prepare the uniform anatase TiO$_2$ nanocrystals with various shapes, which can be tuned from octahedral bipyramid, to truncated octahedral bipyramid, and then to nano-sheet. The ratios between {001} and {101} surface can be easily tuned by changing the amounts of oleic acid and oleylamine. The photocatalytic activity of these anatase TiO$_2$ nanocrystals was also evaluated through the crystal violet photo-degradation under UV light illumination. It was shown that the anatase TiO$_2$ nanocrystals can present the photocatalytic activity comparable to commercial P25.

Introduction

Nowadays, nano-TiO$_2$ has become a key functional material in the fields of photocatalysis, dye-sensitized solar cells (DSSCs), lithium batteries, and the others. [1-10] It was shown that the its properties are closely dependent on the morphologies and the strcuture.[13-19] For example, it was reported that the controllable synthesis of anatase TiO$_2$ nanocrystals with various exposed facets is important for improving the photocatalytic activity. [20-26] From the viewpoint of thermodynamic, anatase TiO$_2$ has the shape of truncated octahedral bipyramid that is surrounded with eight {101} facets and two {001} facets. This is a very popular crystal shape in nature. Moreover, theoretical studies showed that the order of average surface energy is $\gamma\{110\}$ (1.09 J m^{-2}) > $\gamma\{001\}$ (0.90 J m^{-2}) > $\gamma\{100\}$ (0.53 J m^{-2}) > $\gamma\{101\}$ (0.44 J m^{-2}). [27] The high energy {001} facets may be more reactive for dissociative adsorption of reactant molecules than that of the {101} facets, so it was shown that the TiO$_2$ with highly-exposed {001} facets should present better performances for both photocatalysis and DSSCs. [28-31] From this viewpoint, the synthesis of such anatase TiO$_2$ nanocrystals is still interesting for us.

The preparation of anatase TiO$_2$ nanocrystals with highly-exposed {001} facets is difficult as high-energy facets generally diminish during TiO$_2$ nanocrystal growth. [32] Some special surfactants or source materials are needed to prohibit the pre-ferable growth along [101] direction, in order to get nano-TiO$_2$ with highly-exposed {001} facets. After the first synthesis of TiO$_2$ nanocrystals with high-exposed {001} facets from TiF$_4$ solutions through hydrothermal method, [33] much effort have been taken due to their great interest. In additional to pure materials, nitrogen doped anatase TiO$_2$ nanocrystals with highly-exposed {001} facets were also prepared by the hydrothermal treatment of TiN powder in HF solution [31]

Generally, high-concentrated HF solution is needed to grow the anatase TiO$_2$ nanocrystals with highly exposed {101} facets. Lu et al. obtained the anatase TiO$_2$ microcrystals with 64 % {001} facets exposed by using HF as shape controlling agent; [29] this method can be used to further increase the percentage of exposed {001} to 89 %, resulting in the formation of nano-sheets. [34, 35] The big problem is that HF is undesirable due to its high toxicity. The HF-induced TiO_2 nanocrystals also always have large size, which inevitably reduces the specific surface area and limits their applications. In additional to HF, other surfactants were also attempted. For example, Zhao et al. got mesoporous TiO_2 microspheres covered dominantly with {001} facets with using H_2SO_4 as surfactants through hydrothermal method. [36] Xia et al. obtained uniform tiny TiO_2 nanocrystals with exposed {101} facets by treating the electrospinned TiO_2- polyvinylphenol (PVP) complex materials by hydrothermal reaction.[37] It was shown that the shape of TiO_2 nanocrystals depends on the pH. In comparison with the HF-induced method, the TiO_2 nanocrystals prepared by Xia et al. have much smaller size. With diethylenediamine and isopropyl alcohol being used as the surfactants, Chen et al. got the hierarchical spheres that are composed of ultrathin anatase TiO_2 nanosheets with nearly 100 % exposed (001). This material has specific surface area of 170 m^2/g. [38] Do et al. reported a non-aqueous solvothermal method to prepare the anatase TiO_2 nanocrystals with rhombic, truncated rhombic, spherical, and dog-bone shapes. [39] In this method, ethanol, titanium butoxide (TBT), oleic acid (OA), and oleylamine (OM) were used as solvent, titanium precursor, and capping surfactants, respectively. Water vapour was used as the hydrolysis agent of TBT to control the reaction rate.

The controllable growth of TiO_2 nanocrystals with perfect shapes needs low reaction speed, so non-aqueous condition was favorable. However, non-aqueous condition affect product yield of TiO_2 nanocrystals due to low water amount and low reaction speed. From this viewpoint, the development of a green and risk-less hydrothermal method to prepare such TiO_2 materials is necessary and attractive. This needs that the titanium precursor should have low reaction speed. Our previous researches showed that titanium peroxide sol is very stable in air, which can kept for several months.[39, 40] It is a good titanium precursor to grow anatase TiO_2 nanocrystals without using any reaction inhibitors through hydrothermal routine. In the present research, with using OA and OM as the capping surfactants, a facile harmless hydrothermal method was invented to prepare anatase TiO_2 nanocrystals with the exposed {101} facets. The {001}/{101} ratio can be well controlled, and the shapes of the anatase TiO_2 nanocrystals can be tuned from octahedral bipyramids, to truncated octahedral bipyramids, and then to nano-sheets. The application of them in photocatalysis was also studied through the photo degradation of crystal violet (CV) under UV light illumination. It was shown that the anatase TiO_2 nanocrystals present the photocatalytic activity that can be comparable to the commercial P25.

Experimental

Titanium peroxide sol preparation: 8 mL $TiCl_4$ was added in 500 mL ice-cold distilled water (ca. 0-5 °C) under continuous magnetron stirring. Several hours later, the $TiCl_4$ water solution became transparent. Then, 1:5 ammonia was slowly added in the $TiCl_4$ water solution to produce $Ti(OH)_4$ participate until the pH of ca. 7. The $Ti(OH)_4$ sedimentation was kept for ca. 12 h, and then it was filtered and cleaned for several times by the ionized water. The cleaned $Ti(OH)_4$ sedimentation was dispersed in cold distilled water (~4 °C) again, and then 80 mL H_2O_2 was slowly added. The mixed water solution was kept stirring until it became a yellow transparent titanium peroxide sol.

Table 1. Experimental parameters for the preparation of TiO_2 nanocrystals by using hydrothermal method.

	OA (mL)	OM (mL)	Titanium peroxide sol (mL)	Ethanol (mL)
Group-1	2	12	20	33
	5	10	20	33
	8.5	8.5	20	33
	10	5	20	33
	12	2	20	33
Group-2	0	7	20	33
	3	7	20	33
	6	7	20	33
	9	7	20	33
Group-3	7	0	20	33
	7	3	20	33
	7	6	20	33
	7	9	20	33

Synthesis of the TiO_2 nanocrystals: 20 mL yellow titanium peroxide sol was placed in a Teflon-closed steel autoclave. The OA and OM were dissolved in 33 mL ethanol. Afterwards, the OA and OM ethanol solutions were mixed with the titanium peroxide sol in the autoclave, which was then kept stirring for some minutes. The mixed solution was hydrothermally treated at 150 °C for 18 h to get the final product. The amounts of titanium peroxide sol and ethanol were kept unchanged, and the amounts of OA and OM were adjusted for various experiments, which were classified as three groups, as shown in Table 1. Lastly, the TiO_2 products were washed and cleaned by ethanol for several times to remove the physically-adsorbed residual organic surfactant, and then were dispersed in toluene for the further characterization.

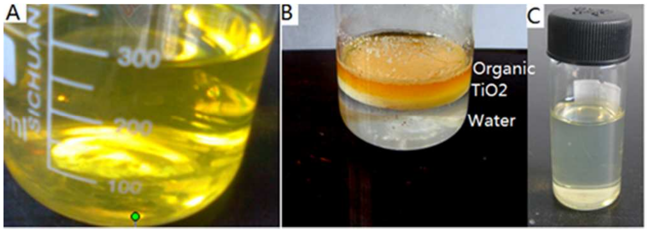

Fig. 1 Digital Pictures of the titanium peroxide sol (A), the mixed solution after hydrothermal treatment (B), and the transparent toluene solution containing as-prepared anatase TiO_2 nanocrystals.

Characterization: X-ray diffraction (XRD) patterns of the anatase TiO2 nanocrystals were checked using a D/Max-IIIA X-ray diffraction meter in a 2θ mode from 10° to 80°. High-resolution transmission electron microscope (HR-TEM) images were observed using a transmittance electron microscopy (HITACHI, H-600 STEM /EDX PV910). The thermo-gravimetric analysis (TG-DTA) was carried out under a flow of air with a temperature ramp of 5 °C min-1 by using a thermal analyser (Germany, NETZSCH, STA449c/3/G). Infrared absorption spectra were recorded by using Nexus fourier transform infrared spectroscopy (FT-IR) in the range of 400-2000 cm-1 (America, Thermo-Nicolet company)

Photocatalytic measurement: Firstly, 0.04 g TiO_2 nanocrystal powders were mixed with ethanol in a ϕ100 glass container, which was then ultrasonically dispersed for ca. 30 min. The ethanol was removed by heated at 70 °C, and then 50 mL crystal violet (CV, 6 mg L^{-1}) was slowly added in the glass container. The adsorption and photocatalytic abilities of the TiO_2 samples were evaluated by measuring the UV-Vis absorption spectra of the CV aqueous solutions for different reaction intervals. A 15 W (TOSHIBA, 365 nm) UV fluorescent lamp was used as light source. The UV light intensity was measured to be ca. 1.0 mW cm^{-2}.

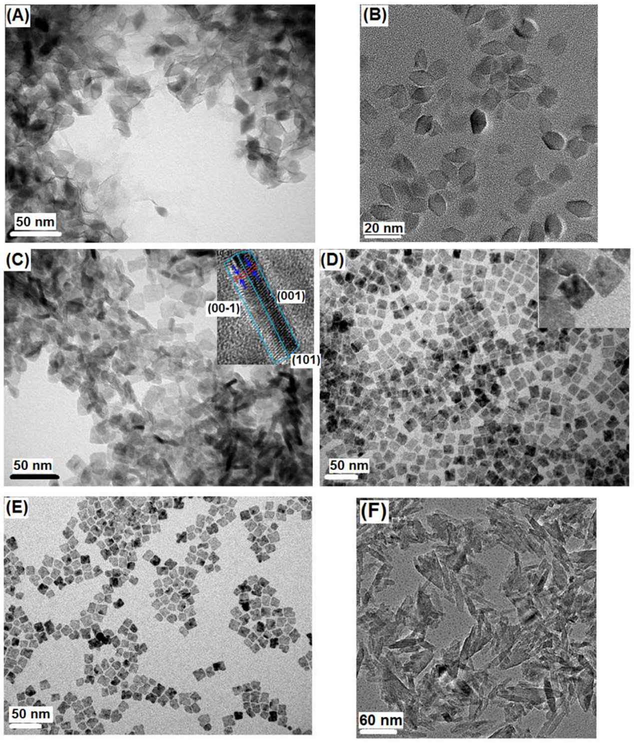

Fig. 2. TEM images of TiO_2 nanocrystals prepared according to group-1: (A) OA: 2 mL, OM : 12mL; (B) OA: 5 mL, OM : 10 mL; (C) OA: 8.5 mL, OM: 8.5 mL; (D) OA : 10 mL, OM : 5 mL; (E) OA : 12 mL, oleylamine 2 mL; (F) TEM image of TiO2 sample prepared by hydrothermal treatment without using OA and OM

Results and discussion

Fig. 1 shows the pictures of the titanium peroxide sol (A), the mixed solution after hydrothermal reaction (B), and the toluene solution that contains the TiO_2 nanocrystals (C).The titanium peroxide sol is a yellow transparent water sol, which is very stable and can be kept for several months at room temperature and air atmosphere. After hydrothermal treatment, it can be seen that the yellow transparent solution changed to a mixture solution with three layers, as shown in **Fig.** 1 (B). The top, middle, and bottom layers are the OA and OM ethanol solution, the white TiO_2 nanocrystal solution, and the water-ethanol solution, respectively. The TiO_2 nanocrystals should be capped with OA and OM molecule, so they are both hydrophobic and oleophilic, which makes the TiO_2 sample locate between the oil and water layers. After the solutions of top and bottom layers were carefully removed, the middle layer that contains the TiO_2 sample was left, which were then washed by ethanol for several times to remove the physically-absorbed OA and OM molecule. The white TiO_2 sample was lastly dispersed in toluene for the further TEM checking, which can form an optical transparent solution, as shown in **Fig. 1** (C).

Fig. 2 shows TEM images of the as-prepared TiO_2 samples prepared according to the parameters of group-1 (Table 1). In these experiments, the OA amount was increased from 2 mL to 12 mL, and the OM amount was decreased from 12 mL to 2 mL. When 2 mL of OA and 12 mL of OM were used, it can be seen from **Fig. 2** (A) that the hydrothermal product is composed of very small uniform TiO_2 nanocrystals, which present the shape of octahedral bipyramids. Obviously, they belong to anatase TiO_2 single nanocrystals. The nanocrystals are surrounded by eight {101} surface, and almost no {001} exposed facets can be seen. The ratio of exposed {001} and exposed {101} is near ca. 0. When the OA amount was increased to 5 mL, and the OM amount was decreased to 10 mL, the hydrothermal product changed to the uniform nanocrystals with the shape of truncated octahedral bipyramids. These TiO_2 nanocrystals contain both exposed {101} and {001} facets (**Fig. 2(B)**). By selecting some nanocrystals, the average ratio between the exposed {001} and the {101} facets was calculated to be ~ 7 %. The further increase of OA amount to 8.5 mL and the further decrease of OM amount to 8.5 mL changed the shape of the hydrothermal sample to nanosheets with the thickness of ca. 6 nm (**Fig. 2 (C)**). The high-resolution TEM image of one stood nanosheet was shown in the top-right corner of this Figure. It can be seen that TiO_2 nanosheet present the shape of truncated octahedrons. The {001}/{101} ratio of this sample is ~ 60 %. The continuous increase of OA amount and decrease of OM amount cannot change the shape of TiO_2 nanocrystals anymore, and they are still in the form of nano-sheets, but their size tends to become smaller. As no stood TiO_2 nano-sheets can be seen, although the thicknesses of these samples cannot be decided, they should be thinner than the sample shown in **Fig. 2 (C)**. For comparison, the sample prepared without using OA and OM is shown **Fig. 2(F)**, and it can be seen the TiO_2 nanoparticles has irregular shape. Therefore, the above results show that the OA and the OM are important to control the shape evolution of TiO_2 nanocrystals even in hydrothermal environments, in additional to the non-aqueous methods. It can be known that the OA tends to control the formation of {101} surface, and OM tends to limit the growth of TiO_2 nano-crystal along [001] direction. As a result, by using the titanium peroxide sol as the titanium precursor, the anatase TiO_2 nanocrystals with the tunable shapes and the controllable {001}/{101} ratio can be prepared by just using a facile hydrothermal method.

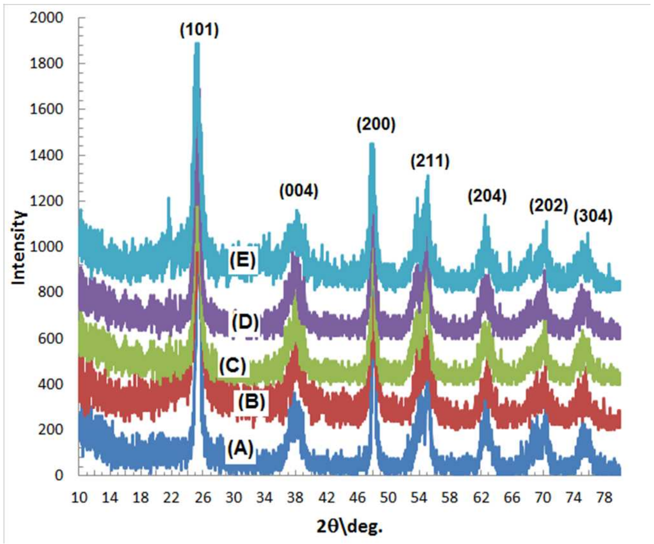

Fig. 3 XRD patterns of TiO_2 nanocrystals prepared according to group-1. (A) OA : 2 mL, OM: 12 mL; (B) OA : 5 mL, OM : 10 mL; (C) OA: 8.5 mL, OM : 8.5 mL; (D) OA : 10 mL, OM : 5 mL; (E) OA ;12 mL, OM : 2 mL

Fig. 3 shows the XRD patterns of the TiO_2 samples prepared according to the experimental parameters of group 1. All of the samples can be indexed as the anatase TiO_2. With the increase of the OA amount and the decrease of OM amount, the X-ray diffractive intensity of (004) lattice becomes weaker and weaker, showing that the thermodynamically preferable growth of TiO_2 nanocrystals along the [001] direction is limited. At the same time, it can be seen that the intensity ratio of (101) peak and (004) peak increase, suggesting that the shape of anatase TiO_2 nanocrystal shape should alter from the octahedral bipyramids, to the truncated octahedral bipyramids, and then to the nano-sheets, which accords to the TEM analysis.

To clearly show the role of OM in the controllable growth of anatase TiO_2 nanocrystals, the OM amount was kept unchanged at 7 mL during hydrothermal reaction, with the OA amount being changed from 0 mL to 9 mL, as shown in Table 1-group-2. **Fig. 4** shows the TEM images of the TiO_2 samples. When the OA was not used, the as-prepared anatase TiO_2 nanocrystals are in the shape of octahedral bipyramids (**Fig.** 4(A)), with less {001} surface being exposed. As the OA amount was increased to 3 mL, the shape of anatase TiO_2 nanocrystals transfers to truncated octahedral bipyramids (**Fig.** 4(B)). One nanocrystal was shown in **Fig. 4(C)**, and the angle labelled is 68.3°, which indicates a good anatase crystalline phase. The magnification of **Fig. 4(C)** is shown in **Fig. 4(D)**, three sets of crystalline facets of anatase were labelled, which are corresponding to (-101), (002), and (101) crystalline lattices of anatase according to XRD analysis, We roughly estimate the percentage of exposed {001} facets of the TiO_2 nanocrystal in **Fig. 3(C)**, which is ca. 8 % . As the OA amount was increased to 6 mL, most of the TiO_2 nanocrystals are nanosheets (**Fig. 4(E)**), although it also contains some truncated octahedral bipyramids. When the OA amount was increased 9 mL, it can be seen from **Fig. 4(F)** that all of TiO_2 nanocrystals are in the shape of nano-sheets. The above results gave us a clear conclusion that OA plays an important role in the formation of the exposed {101} facets under the condition of hydrothermal reactions.

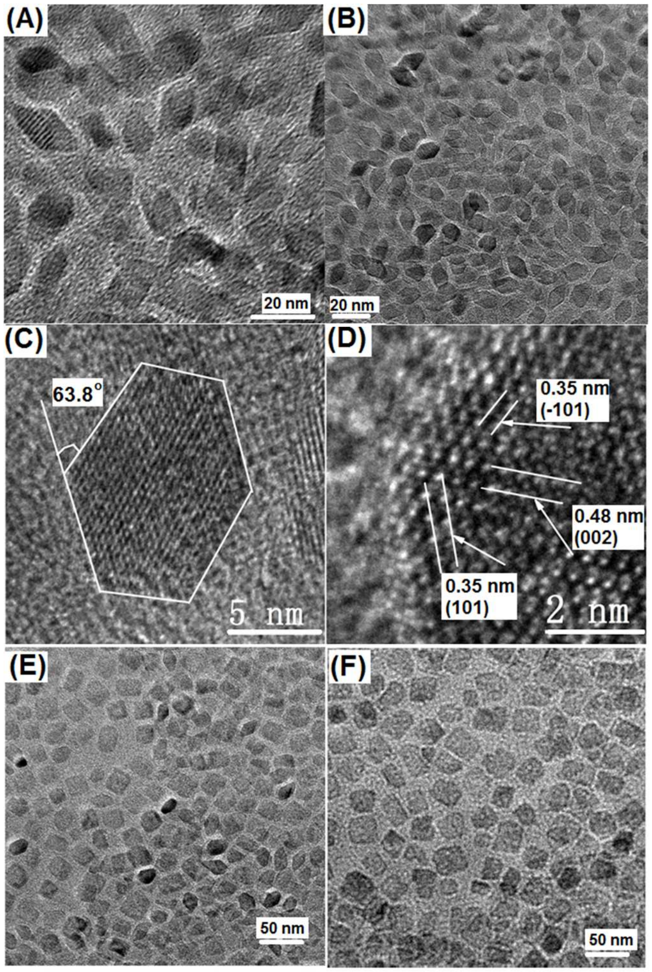

Fig. 4 TEM images of TiO_2 nanocrystals prepared according to group-2: (A) oleic acid 7 mL, oleylamine 0 mL; (B) oleic acid 7 mL, oleylamine 3 mL; (C) oleic acid 7 mL, oleylamine 6 mL; (D) oleic acid 7 mL, oleylamine 9 mL;

Similarly, in order to confirm the function of the OA for preparing the shape-controllable anatase TiO_2 nanocrystals, the OA was kept unchanged at 7 mL, with the OM amount being changed from 0 mL to 9 mL, as shown in Table 1 (group 3). Fig. 5 shows the TEM images of these TiO_2 samples. Differently, it can be seen that all of the anatase TiO_2 nanocrystals are in shape of nano-sheets, almost independent on the OM amount. Therefore, it seems that the OA should have a stronger effect in controlling TiO_2 nanocrystal growth, as compared to the OA, because the use of 9 mL of OM cannot induce the obvious change of TiO_2 nanocrystal shape, which is still in the form of nano-sheets.

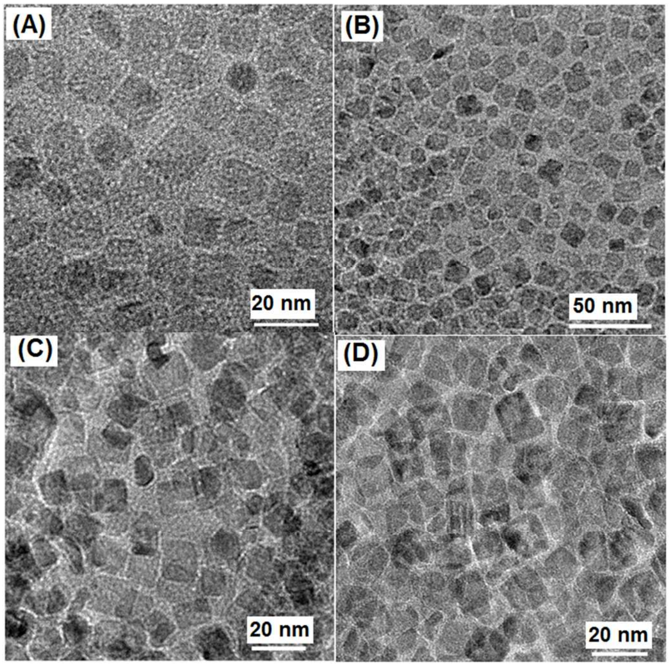

Fig. 5 TEM images of TiO_2 nanocrystals according to group-3. (A) oleic acid 0 mL, oleylamine 7 mL; (B) oleic acid 3 mL, oleylamine 7 mL; (C) oleic acid 6 mL, oleylamine 7 mL; (D) oleic acid 9 mL, oleylamine 7 mL;

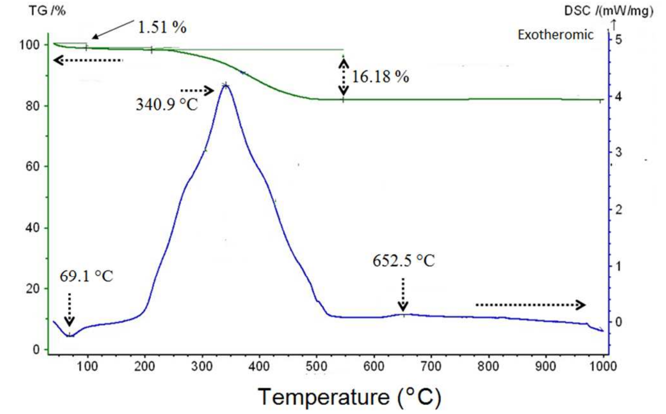

Fig. 6 TG-DTA results of the TiO_2 sample prepared with using 5 mL OA and 10 mL OM

The TiO_2 sample (**Fig. 2 (B)**) was firstly dried at 30 °C, and then was balled as TiO_2 powder for TG-TDA analysis, as shown in **Fig. 6**. The first ~ 1.5 % weight-loss happening at 69.1 °C corresponds to an endothermic process, which is from the evaporation of the organic toluene. The second ~ 16.18 % weight–loss happening at 340.9 °C is an exothermic process, which is corresponding to the decomposition and oxidation of the OA and the OM adsorbed on TiO_2 surface. The exothermic peak at ~ 652.5 °C on the DTA curve is due to the anatase-to-rutile transition as there is no weight-loss at this temperature. In summary, the TG-DTA analysis showed that the TiO_2 sample contains ~16.2 % organic species. The FT-IR spectra of the TiO_2 samples prepared with and without using the OA and the OM are shown **Fig. 7**. If the OM and the OA were used during the hydrothermal treatment, four additional strong adsorption peaks at 1462, 1426, 2852, and 2922 cm^{-1} appear at the spectrum (red line). The FT-IR absorption peak at 1462 cm^{-1} is corresponding to the bending vibration of –CH bond, and the peak at 1526 cm^{-1} is due to the vibration of N-H bond, which indicate the existence of the OM molecule on the TiO_2 nanocrystal surface. In addition, the peaks at 2852 and 1922 cm^{-1} are from the stretching vibration of $–CH_3$, CH_2, or CH groups, also indicating the presence of OA on the TiO_2 surface. In order to remove these surface-capped organics, the TiO_2 sample (**Fig. 2 (B)**) was annealed at 450 °C for an hour, and the TEM image of the annealed TiO_2 sample was shown in **Fig. 8**. Although the annealing process can remove the adsorbed organics, it can be seen that the shape of truncated octahedrons were destroyed.

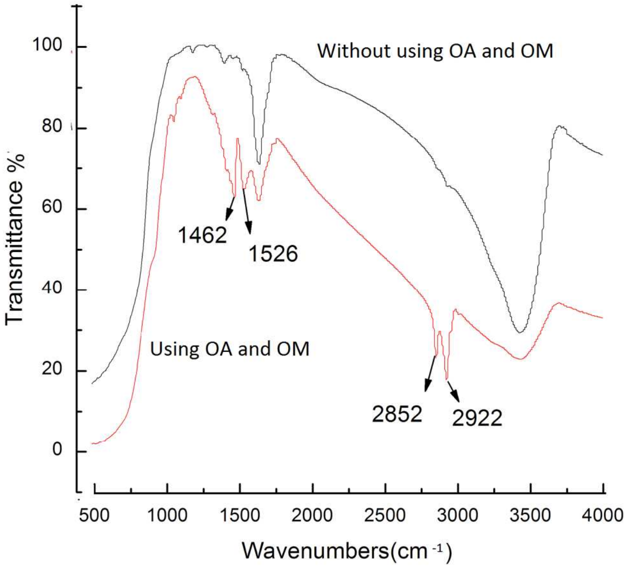

Fig. 7 FT-IR spectra of the TiO_2 samples prepared with using and without using OA and OM in the hydrothermal reactions.

The theory of Wulff construction tells us that the shapes of anatase TiO_2 nanocrystals are mainly controlled by the growth speed along [001] and [101] directions. Due to the high surface energy of {001} surface (0.9 J m^{-2}), anatase TiO_2 nanocrystals generally prefer to grow along the [001] direction, which leads to the disappearing of {001} surfaces. As indicated by our results and other study, [38] the OA molecule should preferably adsorb on {001} surfaces, which prevents the TiO_2 nanocrystal growth along [001] directions, resulting in the formation of octahedral bipyramids. If the OM was also used during the hydrothermal reactions, our above observations indicate that the OM molecule can be preferably and strongly adsorbed on {101} surface, [38] which limits the anatase TiO_2 nanocrystals growth along [101] direction. In this case, the anatase TiO_2 nano-crystals will grow along both [001] and [101] directions, which finally leads to the formation of the truncated octahedral bipyramids and the nano-sheets, as shown in **Fig. 2**. By altering the ratio between the OA amount and the OM amount, the {001}/{101} ratio of anatase TiO_2 nanocrystals can be altered.

Furthermore, our results show that the OA seems to be more highly-functional to control the anatase TiO_2 nanocrystal shape as compared to the OM.

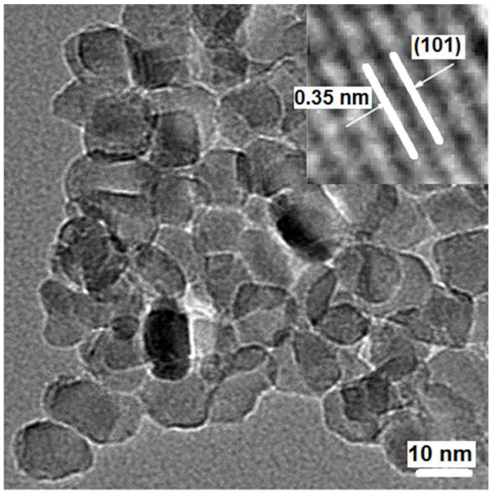

Fig. 8 TEM image of the annealed TiO_2 sample prepared by the hydrothermal treatment with using 5 mL of OA and 10 mL of OM

The other titanium precursors, such as tetrabutyl titanate and titanium isopropoxide, will suffer from the fast hydrolysis during the hydrothermal reaction in the present of much water if no acid is used. The hydrolysed product locates at the bottom of the autoclave, which prevents the good contact among titanium, OA, and OM. This disadvantage limits the accurate controlling of the anatase TiO_2 nanocrystal shape. As we have discussed above, the no-aqueous methods were generally used to prepare these TiO_2 samples. For example, Wu *et al.* used OA and titanium isopropoxide as capping surfactants and titanium precursor to prepare TiO_2 nanosheet and TiO_2 nanocrystals with highly-exposed {001} and {001} facets through the no-aqueous solvothermal method, with tiny water being used as the oxygen source; [34] Dinh *et al*. used tetrabutyl titanate as titanium source to prepare TiO_2 nanocrystals with various shapes through no-aqueous solvothermal method, with the OA and the OM being also used as the capping surfactants. [38] As only low amount of water is allowed during the non-aqueous solvothermal reaction, the controllable growth of anatase TiO_2 nanocrystals can be realized. However, it is difficult to achieve the large-quality production of anatase TiO_2 nanocrystals due to the presence of tiny water. Compared with tetrabutyl titanate and titanium isopropoxide, titanium peroxide sol is much stable, which can be kept for several months without obvious change. Under the heating, titanium peroxide sol slowly decomposes and transfers to titanium oxide clusters, which can be uniformly crystallized during hydrothermal treatment at the natural condition without using the inhibitor to suppress reaction speed. The slow reaction speed allows the anchoring of OA and OM molecule on the TiO_2 cluster surface, which finally controls the shapes of anatase TiO_2 nanocrystals. As much water exists during the hydrothermal reaction, so the reaction speed should be faster than that of the no-aqueous solvothermal method and the high production yield can also be realized. From this viewpoint, the facile hydrothermal method without using the highly-toxic HF to control the anatase TiO_2 nanocrystal shapes is feasible if the titanium peroxide sol is used as the titanium precursor. The formation mechanism of anatase TiO_2 nanocrystals is shown in **Fig. 9**

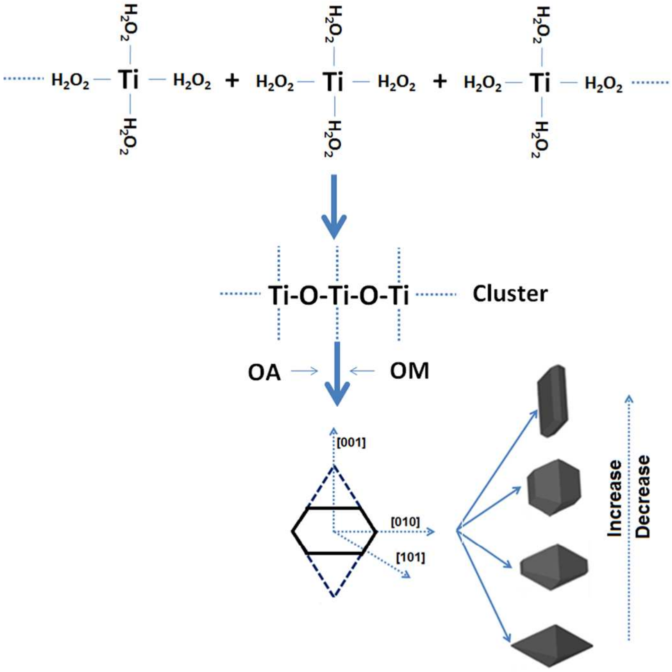

Fig. 9 Diagram of anatase TiO_2 growth along [001] and [101] direction.

The application of such TiO_2 nano-crystals in photocatalysis was evaluated. Three anatase TiO_2 nanocrystal samples with different exposed {001}/{101} ratios were choosen to study the photocatalytic activity, with commercial P25 being used as the reference. Considering that the CV photo degradation is a complicated process in which the adsorption on a TiO_2 surface is the first step, the adsorption experiment was carried out to compare the adsorption ability of different samples. **Fig. 10 (A)** shows the change of CV concentration after different periods of dark adsorption. The adsorption of CV on TiO_2 surface almost reaches the equilibrium after ~2 h. P25 TiO_2 has the lowest adsorption capacity, while the our samples show obvious adsorptions. The adsorption abilities decrease as the {001}/{101} ratio increases. It was considered that the capped surfactants on the anatase TiO_2 nanocrystals should play an important role for CV adsorption.

Fig. 10 (B) shows the dependences of C/C_0 of CV solutions on the time of UV light irradiation. All of the samples present photocatalytic activity. It was observed that the sample with the highest {001}/{101} ratio has the lowest photocatalytic activity, i.e., the photocatalytic activity decreases as the {001}/{101} ratio increases. This result is different from other researches, which reported that highly-exposed {001} facets is favourable for photocatalysis. In the present research, the OA adsorbing on {001} surface of anatase TiO_2 nanocrystals may change the surface energy and structures, which limits the positive function of {001} surfaces. Combined the result of Fig. 10 (A), it was also considered that the adsorption of TiO_2 nanocrystals for CV may also have an effect on the photocatalytic activity, as high adsorption ability can capture more CV molecule on TiO_2 surface. **Fig. 10 (B)** also shows that the photocatalytic activity of our sample can be comparable to commercial P25 TiO_2.

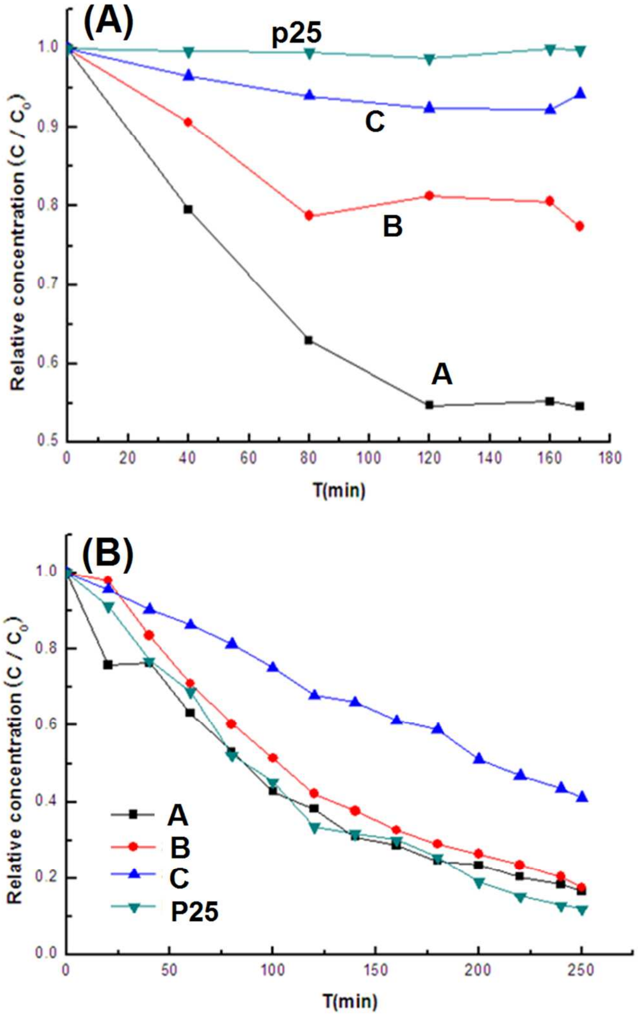

Fig. 10 (A) CV dye adsorption for TiO_2 sample A (OA: 2 mL, OM : 12 mL), B (OA: 5 mL, OM : 10 mL;), C (OA: 8.5 mL, OM: 8.5 mL;), and the commercial P25; (B) their photocatalytic performance in degradation of CV in comparison with the commercial P25

Conclusions

In the present research, with using the titanium peroxide sol as the titanium precursor, a facile and wild hydrothermal method was invented to prepare the anatase TiO_2 nanocrystals with the tunable shapes and the exposed {001}/{101} ratios under the neutral condition. In comparison with other titanium precursor, the titanium peroxide sol is stable in air atmosphere, and it can slowly decomposes and transfer to TiO_2 under the hydrothermal treatment, which is determined for controlling the shapes of the anatase TiO_2 nanocrystals prepared using hydrothermal method. In the photo degradation of CV dyes, the anatase TiO_2 nanocrystals can have the photocatalytic activity comparable to the commercial P25.

Acknowledgements

B. Liu thanks for the Fundamental Research Funds for the Central Universities (Wuhan University of Technology, 2012-IV-008).

Notes and references

[a]State Key Laboratory of Silicate Materials for Architectures Wuhan University of Technology, Luoshi Road 122, Wuhan city, Hubei province, 430070, P. R. China Fax: (+) +86-027-87669729
E-mail: liubaoshun@126.com

[1] Y. Wu, D. Chu, P. Yang,. Y. Dua, C. Lu, *Catal. Sci. Technol.*, 2015, **5**, 3375-3382

[2] X. Li, P. Liu, Y. Mao, M. Xing, J. Zhang, *Appl. Catal. B: Environ.* 2015, **164**, 352–359.

[3] S. Banerjee, D. D. Dionysiou, S. C. Pillaic, *Appl. Catal. B: Environ.* 2015, **176–177**, 396–428

[4] S. Horikoshi, H. Tsutsumi, H. Matsuzaki, A. Furube, A. V. Emeline, N. Serpone, *J. Mater. Chem. C*, 2015,**3**, 5958-5969

[5] J. Schneider, M. Matsuoka, M. Takeuchi, J. Zhang, Y. Horiuchi, M. Anpo, D. W. Bahnemann , *Chem. Rev.*, 2014, **114**, 9919–9986

[6] X. Lang, X. Chen, J. Zhao, *Chem. Soc. Rev.,* 2014, **43**, 473-486

[7] D. M. Schultz, T. P. Yoon, *Science*, 2014, **343**, no. 6174.

[8] M. Wang, J. Ioccozia, L. Sun, C. Lin, Z. Lin, *Energy Environ. Sci.*, 2014, **7**, 2182-2202

[9] S. Banerjee, S. C. Pillai, P. Falaras, K. E. O'Shea, J. A. Byrne., D. D. Dionysiou, *J. Phys. Chem. Lett.*, 2014, **5**, 2543–2554

[10] J. S. DuChene, B.C. Sweeny, A. C. Johnston-Peck, D. Su, E. A. Stach, W. D. Wei, *Angew. Chem. Int. Ed.*, 2014, **53**, 7887-7891.

[11] H. Xu, G. Li, G. Zhu, K. Zhu, S. Jin, *Catal. Comm.* 2015, **62**, 52-56.

[12] X. Chen, L. Liu, P. Y. Yu, S. S. Mao, Science, 2011, 331, 746-750.

[13] S. Liu, J. Yu, M. Jaroniec, *J. Am. Chem. Soc.* 2010, **132**, 11914–11916.

[14] Q. Xiang, J. Yu, M. Jaronie, *Chem. Commun.*, 2011, **47**, 4532–4534

[15] J. Ye, W. Liu, J. Cai, S. Chen, X. Zhao, H. Zhou, L. Qi, *J. Am. Chem. Soc.* 2011, **133**, 933–940.

[16] X. Yu, B. Kim, Y. K. Kim, *ACS Catal.* 2013, **3**, 2479−2486

[17] F. Zuo, L. Wang, T. Wu, Z. Zhang, D. Borchardt, P. Feng, *J. Am. Chem. Soc.* 2010, **132**, 11856–11857

[18]C. Hu, X. Zhang, W.Li, Y. Yan, G. Xi, H. Yang, J. Li, H. Bai, *J. Mater. Chem. A*, 2014, **2**, 2040-2043

[19] J. Zhang, L. Qian, W. Fu, J. Xi, Z. Ji, *J. Am. Ceram. Soc.*, 2014, **97**, 2615–2622.

[20] K. Chen, Z. Jiang, J. Qin, Y. Jiang, R.Li, H. Tang, X. Yang, *Ceram. Intern*, 2014, **40**, 16817–16823.

[21] M.-V. Sofianou, M. Tassi, N. Boukos, S. Thanos, T. Vaimakis, J. Yu, C. Trapalis, *Catal. Today*, 2014, **230**, 125–130.

[22] B. Li, Z. Zhao, F. Gao, X. Wang, J. Qiu, *Appl. Catal. B: Environ.* 2014, **147**, 958-964.

[23] N. Sutradhar, A. K. Biswas, S. K. Pahari, B. Ganguly, A. B. Panda, *Chem. Commun.*, 2014, **50**, 11529-11532.

[24] B. Li, Z. Zhao, Q. Zhou, B. Meng, X. Meng, J. Qiu, *Chem. - Euro. J.* 2014, **20**, 14763–14770.

[25] J. Yu, J. Fan, K. Lv, *Nanoscale* 2010, **2**, 2144–2149.

[26] K. Hou, B. Tian, F. Li, Z. Bian, D. Zhao, C. Huang, *J. Mater. Chem.* 2005, **15**, 2414–2420.

[27] W. Yang, F. Wan, Q. Chen, J. Li, D. Xu, *J. Mater. Chem.* 2010, **20**, 2870–2876.

[28] Y. Zhang, Z. Xie, J. Wang, *ACS Appl. Mater. Interfaces* 2009, **1**, 2789–2795.

[29] H. G. Yang, G. Liu, S. Z. Qiao, C. H. Sun, Y. G. Jin, S. C. Smith, J. Zou, H. M. Cheng, G. Q. Lu, *J. Am. Chem. Soc.* 2009, **131**, 4078–4083

[30] G. Liu, L. Z. Wang, C. H. Sun, X. X. Yan, X. W. Wang, Z. G.Chen, S. C. Smith, H. M. Cheng, G. Q. Lu, *Chem. Mater.* 2009, **21**, 1266.

[31] G. Liu, H. G. Yang, X. Wang, L. Cheng, J. Pan, G. Q. Lu, H. M. Cheng *J. Am. Chem. Soc.* 2009, **131**, 12868–12869

[33] H. G. Yang, C. H. Sun, S. Z. Qiao, J. Zou, G. Liu, S. C.Smith, H. M. Cheng, G. Q. Lu, *Nature* 2008**, 453**, 638.

[34] B. Wu, C. Guo, N. Zheng, Z. Xie, G. D. Stucky, *J. Am. Chem. Soc.* 2008, **130**, 17563

[35] D. Q. Zhang, G. S. Li, X. F. Yang, J. C. Yu, *Chem. Commun.* 2009, 4381.

[36]Z. Zhao, Z. Sun, H. Zhao, M. Zheng, P. Du, J. Zhao, H. Fan, *J. Mater. Chem.*, 2012, **22**, 21965-21971

[37] Y. Dai, C. M. Cobley, J. Zeng, Y. Sun, Y. Xia, Y. *Nano Lett.* 2009, **9**, 2455-2459.

[38] J. S. Chen, Y. L. Tan, C. M. Li, Y. L. Cheah, D. Luan, S. Madhavi, F. Y. C. Boey, L. A. Archer, X. W. Lou, *J. Am. Chem. Soc.* 2010, **132**, 6124–6130.

[39] C.-T. Dinh, T.-D Nguyen, F. Kleitz, T.-O. Do, *ACS Nano*, **2009**, *3*, 3737–3743.

[40] B. Liu, X. Wang, G. Cai, L. Wen, Y. Song, X. Zhao, J. Hazard. Mater. 2009, 169,1112–1118

[41] L. Wen, B. Liu, X. Zhao, K. Nakata, T. Murakami, A. Fujishima, Inter. J. Photoenergy, 2012, Article ID 368750.